

Observation of MnP magnetic clusters in room-temperature ferromagnetic semiconductor $Zn_{1-x}Mn_xGeP_2$ using nuclear magnetic resonance

Taesoon Hwang, Jeong Hyun Shim, and Soonchil Lee

Citation: *Appl. Phys. Lett.* **83**, 1809 (2003); doi: 10.1063/1.1605260

View online: <http://dx.doi.org/10.1063/1.1605260>

View Table of Contents: <http://apl.aip.org/resource/1/APPLAB/v83/i9>

Published by the [American Institute of Physics](http://www.aip.org).

Additional information on *Appl. Phys. Lett.*

Journal Homepage: <http://apl.aip.org/>

Journal Information: http://apl.aip.org/about/about_the_journal

Top downloads: http://apl.aip.org/features/most_downloaded

Information for Authors: <http://apl.aip.org/authors>

ADVERTISEMENT



Goodfellow
metals • ceramics • polymers • composites
70,000 products
450 different materials
small quantities fast

www.goodfellowusa.com

Observation of MnP magnetic clusters in room-temperature ferromagnetic semiconductor $\text{Zn}_{1-x}\text{Mn}_x\text{GeP}_2$ using nuclear magnetic resonance

Taesoon Hwang,^{a)} Jeong Hyun Shim, and Soonchil Lee

Department of Physics, Korea Advanced Institute of Science and Technology,
Daejeon 305-701, South Korea

(Received 2 June 2003; accepted 27 June 2003)

We investigated chalcopyrite $\text{Zn}_{1-x}\text{Mn}_x\text{GeP}_2$ polycrystals, which have been reported as a room-temperature ferromagnetic semiconductor, with Mn concentrations of $x = 0.08$ and 0.15 using ^{55}Mn and ^{31}P nuclear magnetic resonance spectroscopy. The samples were made by the same process and showed the same crystallographic and magnetic behavior as in the previous report, but the experimental results indicated that more than 90% of Mn atoms were in a MnP impurity phase and the MnP cluster size was tens of nanometers. No evidence of Mn atom substitution in the host ZnGeP_2 lattice was observed and the magnetic property of $\text{Zn}_{1-x}\text{Mn}_x\text{GeP}_2$ was determined to be that of the MnP magnetic clusters, at least in the bulk. The inconsistency of the conclusions with x-ray diffraction data is a result of the weak crystallinity of MnP phase. © 2003 American Institute of Physics. [DOI: 10.1063/1.1605260]

A material having both ferromagnetic and the semiconducting properties is potentially very useful in spintronics, where spins are used to process information. A recent approach to practical ferromagnetic semiconductors was the diluted magnetic semiconductor (DMS), where transition-metal ions substitute the cations of the host semiconductor. III–V DMS, such as $\text{In}_{1-x}\text{Mn}_x\text{As}$ or $\text{Ga}_{1-x}\text{Mn}_x\text{As}$, triggered study of the physics of ferromagnetism in DMS, because the creation of spin-polarized p -type carriers elevate T_c to 110 K.¹ Ferromagnetism has also been found in ternary compounds and oxide-based DMSs. Among them, cobalt doped-titanium dioxide $\text{Ti}_{1-x}\text{Co}_x\text{O}_2$ (Ref. 2) and Mn-doped chalcopyrite semiconductors such as $\text{Cd}_{1-x}\text{Mn}_x\text{GeP}_2$ or $\text{Zn}_{1-x}\text{Mn}_x\text{GeP}_2$ (Refs. 3–5) have been reported to show room temperature ferromagnetism.

Various experiments have been conducted to investigate these DMS materials. The magnetic property, especially ferromagnetism in DMS, has been cited mostly based on magnetization measurements. Since these types of macroscopic measurements cannot determine whether a measured property is intrinsic, controversy has arisen over the characteristics of DMS, such as the mechanism of the ferromagnetism. In this work, we report the zero-field nuclear magnetic resonance (NMR) measurement on ferromagnetic DMS samples. NMR can provide valuable information on the microscopic magnetic properties in these semiconductors. In NMR, resonance frequency is proportional to the local field, which is the sum of external and internal fields. The internal field at a nucleus of a magnetic ion in magnetic materials is usually much stronger than the external field. Therefore, the field generated inside due to magnetic ordering is exactly measured by zero-field NMR. NMR of nonmagnetic ions also provides evidence of magnetic ordering, because its resonance frequency is shifted by the internal field in ordered states.

The samples assessed are Mn-doped II–VI–V₂ chal-

copyrite semiconductor $\text{Zn}_{1-x}\text{Mn}_x\text{GeP}_2$ polycrystals with $x = 0.08$ and 0.15 . Medvedkin *et al.* reported room temperature ferromagnetism in highly doped chalcopyrite $\text{Cd}_{0.8}\text{Mn}_{0.2}\text{GeP}_2$,³ and it was later claimed that $\text{Zn}_{1-x}\text{Mn}_x\text{GeP}_2$ is also ferromagnetic at room temperature.^{4,5} This material shows phase transitions from antiferromagnetic to ferromagnetic states at 47 K and ferromagnetic to paramagnetic states around 310 K. Our experimental results, however, strongly indicate that the magnetic property of bulk polycrystalline $\text{Zn}_{1-x}\text{Mn}_x\text{GeP}_2$ is extrinsic. The resonance frequency and line shape of both the magnetic and nonmagnetic ions verify the existence of MnP magnetic clusters, but no evidence of intrinsic ferromagnetism was observed.

Bulk polycrystalline chalcopyrite $\text{Zn}_{1-x}\text{Mn}_x\text{GeP}_2$ was made by the vertical gradient solidification method following Cho *et al.*'s synthesis procedure using the same method and under the same conditions.⁵ We also made a MnP polycrystalline sample, which is the most probable magnetic impurity phase in this case, by a similar procedure. The sample crystallography was studied by θ - 2θ x-ray powder diffraction (XRD) and magnetization was measured by a superconducting quantum interference device (SQUID) magnetometer in a 100 Oe magnetic field. For NMR measurement, spin echo techniques were used with our homemade spectrometer.

Figure 1 displays the diffraction pattern of the 15% sample, where the peaks index with a chalcopyrite structure. The structure of the host material ZnGeP_2 remains the same after Mn doping, and impurity phase is invisible within experimental error. The inset of Fig. 1 shows the diffraction data of a MnP sample that has B-31 type orthorhombic structure⁶ for comparison. The diffraction pattern of the 8% sample is qualitatively the same. The temperature dependence of the magnetization showed an antiferromagnetic to ferromagnetic phase transition at 47 K and a ferromagnetic to paramagnetic phase transition at 300 K. These confirm that the structural and magnetic properties of our samples are identical with those of Cho *et al.*

The hyperfine fields at nuclear sites were calculated us-

^{a)}Electronic mail: htaesoon@mrm.kaist.ac.kr

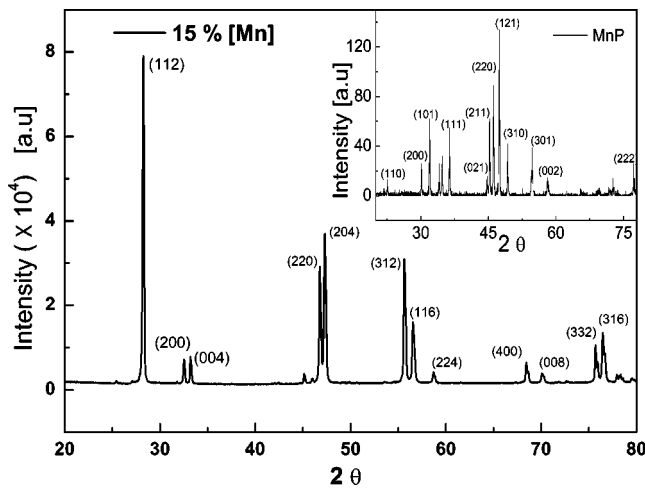


FIG. 1. Powder XRD pattern of the $Zn_{1-x}Mn_xGeP_2$ polycrystalline sample with Mn concentration $x=0.15$. Magnetic impurity phase such as MnP is not seen. The inset shows the XRD data of the MnP sample for comparison.

ing first principle calculations.⁷ According to the calculation, the local field at Mn nuclei is expected to be 55 kOe and that at P nuclei 10 kOe. The corresponding resonance frequencies are 57 and 78 MHz for Mn and P nuclei, respectively. We searched for the NMR signal over a wide range around these resonance frequencies in zero-field NMR but could detect nothing. The only signal observed was at 116 MHz for Mn nuclei and at 74 MHz for P nuclei (Fig. 2). The observed resonance frequency of P nuclei seems close to the theoretical prediction while that of Mn is far from the theoretical value. However, these frequencies are the resonance frequencies of bulk magnetic MnP. The zero-field NMR spectra we obtained from the polycrystalline MnP sample overlap those of $Zn_{1-x}Mn_xGeP_2$, as shown in Fig. 2. Figure 2 shows that not only the resonance frequencies but also the linewidths and even peak splitting of MnP and $Zn_{1-x}Mn_xGeP_2$ samples are the same, irrespective of x . The zero-field NMR spectra of MnP have two peaks for each nuclear spin. The center frequencies are 116 and 142 MHz for Mn nuclei and 70 and 74 MHz for P nuclei. The high frequency peak in the Mn spectrum and the low frequency peak in the P spectrum are

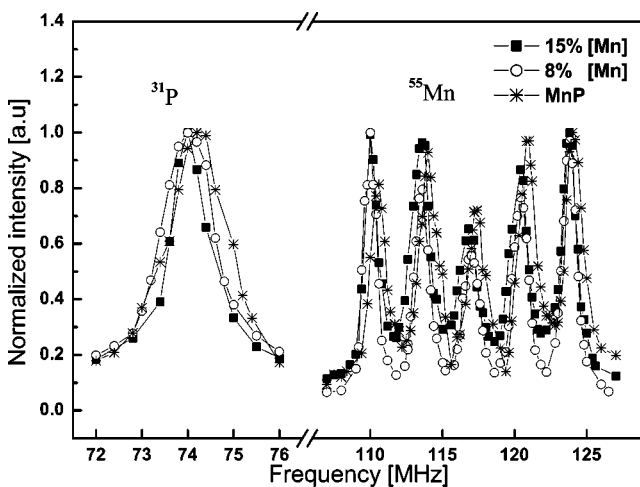


FIG. 2. Zero-field NMR spectra of ^{55}Mn nuclei and ^{31}P nuclei observed at liquid nitrogen temperature for $Zn_{1-x}Mn_xGeP_2$ with $x=0.08, 0.15$ and MnP samples.

usually invisible in a spin echo technique due to their short T_2 relaxation time.⁸ The remaining peaks of MnP are shown in Fig. 2.

In magnetic materials, local fields are generated at nuclei due to the hyperfine interaction between nuclear spins and ordered electron spins. In the case of magnetic ions, the main contribution to the local field comes from the contact hyperfine interaction with s electrons that are polarized by the exchange interaction with the unpaired electrons in the $3d$ shell. Therefore, the resonance frequency of zero-field NMR is sensitive to physical and chemical configurations of s and d electrons such as conductivity and structure. The main contribution to the local field at nonmagnetic P ions is the transferred hyperfine field, which is generated by the spins of s -shell or p -shell electrons polarized by the exchange interaction with the $3d$ electrons of neighboring magnetic Mn ions. Therefore, the local field of nonmagnetic ions strongly depends on the chemical bonding with magnetic ions. MnP is an intermetallic compound of orthorhombic structure, while $Zn_{1-x}Mn_xGeP_2$ is a semiconductor of chalcopyrite structure. This means that the s electron state and the environment around the $3d$ electron of Mn atoms in MnP are quite different from those of $Zn_{1-x}Mn_xGeP_2$. Therefore, if Mn atoms are substituted into Zn sites in $ZnGeP_2$, their resonance frequency cannot be identical to that of MnP. The line broadening and peak splitting of the Mn spectrum also indicate that the Mn atoms in the $Zn_{1-x}Mn_xGeP_2$ sample are in MnP phase. The Mn spectrum splits into five peaks because the degeneracy of spin $5/2$ states of Mn nuclei is removed by interaction with the internal electric field gradient. Therefore, the same amount of splitting in the MnP and $Zn_{1-x}Mn_xGeP_2$ samples means that the crystal fields around the Mn ions in the $Zn_{1-x}Mn_xGeP_2$ sample are the same as those in MnP. Similarly, the P spectrum indicates that the environment around P ions in the $Zn_{1-x}Mn_xGeP_2$ is the same as that of MnP, including the bonding with Mn ions. Summing up, the observed spectra of $Zn_{1-x}Mn_xGeP_2$ clearly arise from MnP magnetic clusters formed inside the sample.

The amount of the embedded MnP clusters can be estimated by comparing the integrated area of the P spectra of $Zn_{1-x}Mn_xGeP_2$ and MnP. Since the signal enhancement factors of both samples were the same, the spectral area is simply proportional to the number of nuclei. The result of analysis shows that more than 90% of Mn atoms of both $Zn_{1-x}Mn_xGeP_2$ samples are in MnP phase.

We also studied P NMR in an external magnetic field of 7 T. Figure 3(a) shows the spectra measured above and below T_c for $x=0.15$. The spectra of the 8% sample are quite similar. The observed center frequency of 121.6 MHz is the resonance frequency expected in a 7 T field. That is, the spectra in Fig. 3 arises from the P ions that are not tied with the polarized Mn ions. The center frequency decreases and the linewidth becomes broader as the temperature decreases below T_c . The linewidths are 70 and 30 kHz at 285 and 375 K, respectively, which are broader than that of pure $ZnGeP_2$ at room temperature (5.5 kHz). This line broadening shrinks to 1.15 kHz without any remaining satellites at the wings of the fundamental spectral line when the magic angle spinning (MAS) technique is applied. This suggests that the line broadening is not related to the transferred hyperfine interac-

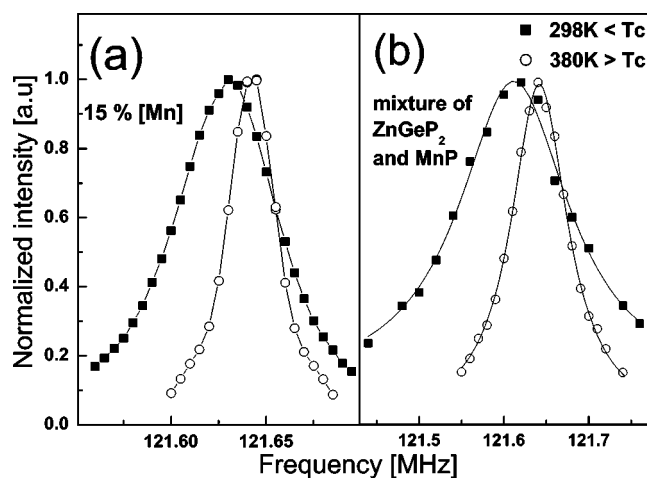


FIG. 3. ^{31}P NMR spectra measured in 7 T magnetic field. (a) Spectrum obtained from the $\text{Zn}_{1-x}\text{Mn}_x\text{GeP}_2$ sample with $x=0.15$ and (b) spectrum of the mixture of ZnGeP_2 and MnP.

tion as expected, because MAS removes only the dipolar broadening.⁹ The local magnetic field corresponding to the center frequency shift is too weak to be explained by the transferred hyperfine field. The local field estimated from the shift is only 6 Oe, while the transferred hyperfine field is usually 10^4 – 10^5 Oe.¹⁰ Both the frequency shift and the line broadening are explained well by the dipolar field generated from MnP magnetic clusters that are saturated at 7 T.

To confirm our conclusion, we observed P NMR for a mixture of pure ZnGeP_2 and MnP powders under the same conditions. The powders were mixed in a jade bowl for 5 h and they were not heat treated. The molar ratio of ZnGeP_2 and MnP is 3:1. The spectra obtained above and below T_c are shown in Fig. 3(b). It is clearly seen that the center frequency shift, linewidth, and overall line shape of the mixed sample are qualitatively the same as those of the $\text{Zn}_{1-x}\text{Mn}_x\text{GeP}_2$ sample at both temperatures. The result of this experiment strongly supports the existence of MnP magnetic clusters inside our $\text{Zn}_{1-x}\text{Mn}_x\text{GeP}_2$ polycrystals.

It is worthwhile to note that MnP also shows transitions from paramagnetic to ferromagnetic and ferromagnetic to antiferromagnetic states at similar temperatures (292 and 50 K).⁶ This quantitative agreement of transition temperatures also supports our findings. Considering that the transition temperatures of magnetic particles depend on size, the particle size of the MnP clusters is estimated to be not so small as to change the bulk property. Another estimate of the average particle size is provided by the enhancement factor in NMR. In ferromagnetic NMR, generally both the signal and rf input are enhanced due to the accompanying oscillation of electronic magnetic moments. The enhancement factor is usually 10 – 10^2 in domains and 10^2 – 10^4 in domain walls.¹⁰ In our experiments, the enhancement factors of bulk MnP and $\text{Zn}_{1-x}\text{Mn}_x\text{GeP}_2$ samples were the same. This means that

the size of the MnP clusters is sufficiently large to have domain walls, because most of the signal of the bulk MnP should come from domain walls. Therefore, the average MnP particle size is at least tens of nanometers. This is, however, inconsistent with the XRD measurement where the MnP phase is not seen. The XRD data of the MnP sample shown in the inset of Fig. 1 suggest an explanation. We have grown this MnP sample under the same conditions with $\text{Zn}_{1-x}\text{Mn}_x\text{GeP}_2$ as stated above. Since the growth conditions of $\text{Zn}_{1-x}\text{Mn}_x\text{GeP}_2$ are very different from those of MnP, the MnP sample is not likely to form good crystallinity. The weak crystallinity of the MnP sample is reflected in the XRD data. The amount of $\text{Zn}_{1-x}\text{Mn}_x\text{GeP}_2$ and MnP samples used for the XRD experiment as identical, but the x-ray intensity of MnP is one order of magnitude smaller. Therefore, the overall x-ray sensitivity of the MnP clusters in the 15% $\text{Zn}_{1-x}\text{Mn}_x\text{GeP}_2$ sample should be 1.5% at most, consistent with experimental observation.

In conclusion, all data obtained in our experiments confirm that the magnetic property of our $\text{Zn}_{1-x}\text{Mn}_x\text{GeP}_2$ samples, which were made by the same process and showed the same crystallographic and magnetic behaviors as those in the previous report, is due to MnP impurity phase, at least in the bulk. The zero-field NMR spectra of both magnetic and nonmagnetic ions overlap those of MnP at the same resonance frequencies. The linewidth and resonance frequency shift of P NMR cannot be explained by the transferred hyperfine interaction with the ordered Mn ions, but instead by the dipolar field of MnP clusters. The analysis of NMR intensity and enhancement factor shows that more than 90% of Mn atoms of $\text{Zn}_{1-x}\text{Mn}_x\text{GeP}_2$ samples are in MnP phase and the cluster size is at least tens of nanometers. The inconsistency of the conclusion concerning XRD data is explained by the weak crystallinity of MnP clusters. No evidence of Mn atom substitution in ZnGeP_2 was observed.

The authors acknowledge support of this work by the NRL program and KOSEF via eSSC at POSTECH.

¹H. Ohno, *Science* **281**, 951 (1998).

²Y. Matsumoto, M. Murakami, T. Shono, T. Hasegawa, T. Fukumura, M. Kawasaki, P. Ahmet, T. Chikyow, S. Koshihara, and H. Koinuma, *Science* **291**, 854 (2001).

³G. A. Medvedkin, T. Ishibashi, T. Nishi, K. Hayata, Y. Hasegawa, and K. Sato, *Jpn. J. Appl. Phys., Part 2* **39**, L949 (2000).

⁴K. Sato, G. A. Medvedkin, T. Nishi, Y. Hasegawa, R. Misawa, K. Hirose, and T. Ishibashi, *J. Appl. Phys.* **89**, 7027 (2001).

⁵S. Cho, S. Choi, G. B. Cha, S. C. Hong, Y. Kim, Y. J. Zhao, A. J. Freeman, J. B. Ketterson, B. J. Kim, Y. C. Kim, and B. C. Choi, *Phys. Rev. Lett.* **88**, 257203 (2002).

⁶E. E. Huber and D. H. Ridgley, *Phys. Rev.* **135**, A1033 (1964).

⁷S. C. Hong (private communication).

⁸H. Nagai, T. Hihara, and E. Hirahara, *J. Phys. Soc. Jpn.* **29**, 622 (1970).

⁹K. Beshah, P. Becla, R. G. Griffin, and D. Zamir, *Phys. Rev. B* **48**, 2183 (1993).

¹⁰E. A. Turov and M. P. Petrov, *Nuclear Magnetic Resonance in Ferro- and Antiferromagnets* (Halsted, New York, 1972).